Pergamon

Cement and Concrete Research 30 (2000) 1057–1062

CEMENT AND CONCRETE RESEARCH

Electrical characterization of aluminous cement at the early age in the 10 Hz–1 GHz frequency range

Youssef El Hafiane[a], Agnès Smith[a,*], Jean Pierre Bonnet[a], Pierre Abélard[b], Philippe Blanchart[a]

[a]*GEMH, Ecole Nationale Supérieure de Céramique Industrielle (ENSCI), 47 a 73 Avenue Albert Thomas, 87065 Limoges Cedex, France*
[b]*SPCTS, Ecole Nationale Supérieure de Céramique Industrielle (ENSCI), 47 a 73 Avenue Albert Thomas, 87065 Limoges Cedex, France*

Received 15 July 1999; accepted 13 April 2000

Abstract

A CFA cement from Lafarge prepared at 20°C, 100% relative humidity, and with water-to-cement weight ratio (W/C) = 0.4, has been tested electrically between 10 Hz–1 MHz and 1 MHz–1 GHz. The samples have been measured at 20°C and 50% relative humidity from 8 h up to 150 h after mixing the water with the cement. For the first frequency range, the results presented here focus on the effect of the chemical nature of the electrode on the electrical response of the cement. Different electrode materials, namely, silver, gold or an indium–gallium mix, have been investigated. Silver leads to a major contribution of the cement–electrode interface to the global electrical response. This effect is less pronounced with gold and indium–gallium. Concerning the higher frequency range, measurements between 1 MHz and 1 GHz enable the evolution of the interface between cement and water during hydration to follow. An analysis of electrical data, namely, the permittivity and the conductivity, has been carried out using a procedure based on a continuous distribution of time constants. The corresponding relaxation frequencies are presented and related to the state of water inside the cement material. A comparison of the electrical behaviour between a cement and a silico-aluminous ceramic, in which water is not as reactive as in a cement, is also discussed.

Keywords: Calcium aluminate cement; Cement paste; Electrical properties; High frequency measurements

1. Introduction

Electrical measurements as a function of frequency is an experimental approach which is used to characterize the response of ceramic materials such as ionic conductors [1], capacitors [2], semiconductors [3] or cements [4–20]. One of the methods reported in the literature is based on impedance spectroscopy, usually in the Hz–MHz range. For a typical ceramic, which consists of grains separated by grain boundaries, coated with electrodes, this technique permits assessment of the various contributions to the global electrical response of the tested material [21]. More recently, high frequency measurements (1 MHz–1 GHz) have been successfully carried out to characterize the solid–liquid interfaces in concentrated ceramic suspensions [22]. In this case, it is possible to follow how the adsorption of molecules such as ligands or dispersants operates at the scale of the powder surface. The dielectric behaviour of hardened cementitious materials after 1 year immersion in a saturated lime solution has also been examined by high frequency measurements [7,8,12,16].

In this paper, we discuss the electrical behaviour in the 10 Hz–1 GHz range of aluminous cement samples at the early age. We wish to show how it is possible to identify either the electrical response of interfaces between cement and electrodes or the dielectric signal of water, which reacts with the cement. For comparison, we also present the electrical response of a porous silico-aluminous material, which does not react chemically with water as a cement does, and in which pores have been filled with water.

2. Experimental procedure

In order to cover from 10 Hz to 1 GHz, two different apparatus have been used. In the 10 Hz–2 MHz frequency

* Corresponding author. Tel.: +33-555-45-22-04; fax: +33-555-79-09-98.
E-mail address: a.smith@ensci.fr (A. Smith).

0008-8846/00/$ – see front matter
PII: S0008-8846(00)00285-4

range, measurements are carried out with an impedance analyser (apparatus: SOLARTRON 1260 from SCHLUMBERGER). It involves applying a sinusoidal voltage, $V(t)$, to the sample, previously coated with electrodes, and recording the flowing current, $I(t)$, which has a phase difference with respect to the voltage. $V(t)$ and $I(t)$ are related by Ohm's law as in Eq. (1):

$$V(t) = I(t)Z^*(\omega) \tag{1}$$

where $Z^*(\omega)$ is the frequency dependant complex impedance. From $Z^*(\omega)$, it is possible to deduce the admittance $Y^*(\omega)$, since:

$$Y^*(\omega) = \frac{1}{Z^*(\omega)}. \tag{2}$$

The complex dielectric permittivity, $\varepsilon^*(\omega)$, of the specimen under test is given by:

$$\frac{Y^*(\omega)}{i\omega} = \varepsilon^*(\omega)K = \varepsilon_0 K(\varepsilon'_R - i\varepsilon''_R) \tag{3}$$

where K is a geometrical factor; ε_0 is the permittivity of vacuum; and ε'_R, ε''_R, the real and imaginary parts of the relative permittivity, respectively. The real part of the conductivity, $\sigma\prime$, is calculated as follows:

$$\sigma' = \frac{Y'(\omega)}{K} = \varepsilon_0 \varepsilon''_R \omega. \tag{4}$$

$Y'(\omega)$ corresponds to the real part of the admittance. The plots presented in this paper are ε'_R and σ' as a function of frequency.

For measurements between 1 MHz and 1 GHz, the technique is different from the vector–voltage–current ratio. It consists of measuring the reflection coefficient of an electromagnetic wave sent on the tested sample (apparatus: 4291 A from HEWLETT-PACKARD). It should be noted that this technique does not imply electrode coverage of the sample under test. It only requires that the specimen presents mirror like faces. The apparatus applies a measurement frequency test signal to the sample, which is terminated at the test port and detects the vector–voltage ratio of the reflected wave, V_{ref}, to the incident wave, V_{inc}. From this ratio, the complex reflection coefficient, $\Gamma^*(\omega)$, is defined as in Eq. (5):

$$\Gamma^*(\omega) = \frac{V_{ref}}{V_{inc}} = \Gamma_x + j\Gamma_y. \tag{5}$$

$\Gamma^*(\omega)$ is related to $Z^*(\omega)$ by Eq. (6):

$$Z^*(\omega) = Z_O \frac{1 + \Gamma^*(\omega)}{1 - \Gamma^*(\omega)} \tag{6}$$

where Z_O is the characteristic impedance of the coaxial line (50 Ω). Knowing the impedance of the sample, it is possible to deduce ε'_R and σ' from Eqs. (2)–(4).

The validity of the two measurement techniques has been checked with two dense ceramic materials, namely, 98% dense alumina (AL23 from DEGUSSA) and 98% dense titanium oxide (TI 603200 from GOODFELLOW). The tested samples are under the form of disks (diameter: 20 mm; thickness: 5 mm for measurements between 10 Hz and 2 MHz, and 2.5 mm for measurements between 1 MHz and 1 GHz). Prior to electrical characterization, the disks are polished down to 1 μm with alumina powder in order to obtain mirror like surfaces. For low frequency measurements, the two opposite flat faces of the disk are coated with silver paste. The values for ε'_R deduced from electrical characterization are constant between 10 Hz and 1 GHz for both samples and equal to 8.5 and 85 for alumina and titanium oxide, respectively. These figures are in accordance with literature data [23] and are truly representative of the specimen under test. No stray effects due to the electrodes, for instance, at low frequencies, or coming from multiple reflections of the electromagnetic waves at high frequencies [22] perturb the measurements.

Concerning the aluminous cement, it is a CFA product from Lafarge. It is mixed with distilled water, with a water-to-cement weight ratio, W/C, equal to 0.4. After mixing the adequate amounts of cement and water for 1 min with a blender, the paste is simultaneously vibrated and de-aerated under very low pressure (10^{-1} atm) for 2 min. This duration is sufficiently low and the quantity of paste large enough so that no significant water evaporation occurs during this air removal step. The fresh paste is cast in cylindrical moulds, which have mirror like faces. The diameter of the mould is 20 mm. The samples are left to cure at 20°C for $t_0 = 8$ h and in 100% relative humidity. The height of the obtained cylinder is at least equal to 6 mm for measurements between 10 Hz and 2 MHz and ranges from 2.5 to 3 mm for measurements between 1 MHz and 1 GHz. The electrical tests are carried out at 20°C, 50% relative humidity and different times, t_1. Though these experimental conditions can induce a moisture gradient in the specimen, it should not dramatically affect the electrical response. In fact, free water relaxes at 20 GHz [16] and this relaxation should only slightly affect the electrical signal around 1 GHz. The times reported on the various figures refer to the total time, $t_0 + t_1$ after mixing. Prior to characterization at low frequencies, the cement cylinders are coated with either silver electrodes, or gold (deposited by sputtering) or a eutectic mix of 25 wt.% indium–75 wt.% gallium [24]. Gold and indium–gallium mix have been chosen because they are used as electrode materials in microelectronics and are known to give better electrical contacts than silver electrodes [25].

A silico-aluminate ceramic which has 31 vol% of porosity has also been characterized in the high frequency range. The experiment we wish to conduct with this sample, which does not react with water as cement does, is to partly fill up the pores with controlled amounts of water and measure the corresponding dielectric response at high frequencies. The sample is a disk with the following dimensions: thickness 2 mm and diameter 20 mm.

3. Results and discussion

Fig. 1 shows the variations of ε'_R (Fig. 1a) and σ' (Fig. 1b) as a function of frequency in the 10 Hz–2 MHz range for the aluminous cement where $t_0 + t_1 = 150$ h. The following comments can be made: (i) the variations of ε'_R and σ' are clearly dependent on the chemical nature of the electrode; (ii) for Au and In–Ga coated surfaces, σ' remains fairly constant up to 10 kHz and starts raising afterwards. In the case of the Ag coated material, σ' always increases (Fig. 1b); (iii) ε'_R decreases regularly with frequency (Fig. 1a); (iv) the value of ε'_R especially at the lowest frequency end is very high compared to what has been recorded on systems such as wetted rocks. For instance, in basalt, whose porosity is partly filled with physically adsorbed water, the remainder being filled with air, ε'_R measured at 10 Hz has values which increase between 6.9 and 8.8 when the water content goes from 0 to 0.15 wt.% [26]. Another illustration is given by sandstone [27]. When the number of water layers adsorbed in the porosity goes from 0 to 4, which corresponds to approximately 1-nm thick, ε'_R at 105 kHz raises from 6 to 28 and remains fairly constant up to the saturation of pores (i.e. 30 adsorbed layers).

In order to understand the general shape of the curves on Fig. 1, one possible approach is to schematically represent

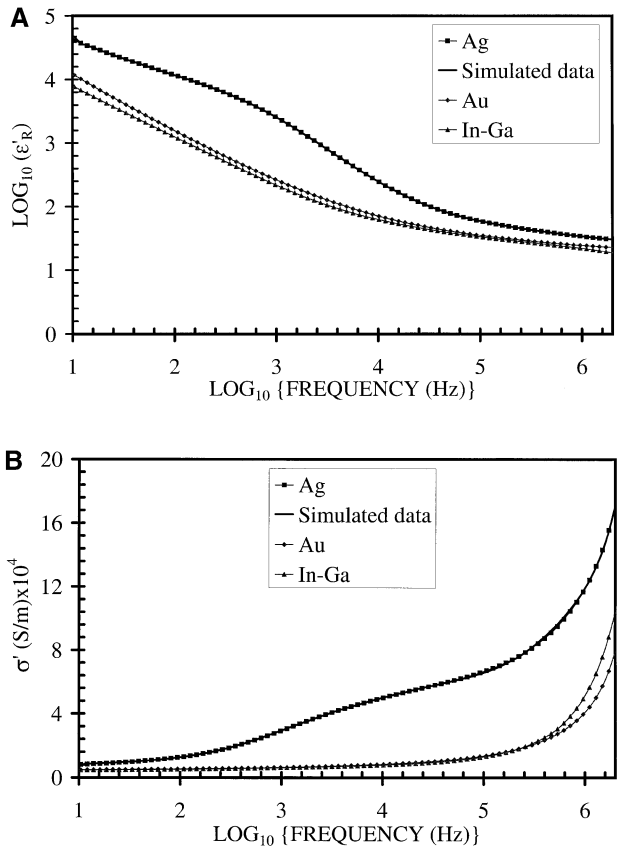

Fig. 1. Variations of ε'_R (a) and σ' (b) as a function of frequency in the 10 Hz–2 MHz range for the aluminous cement ($t_0 + t_1 = 150$ h).

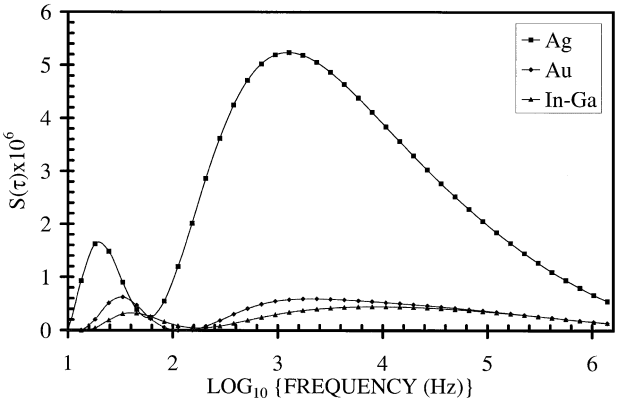

Fig. 2. Variations of $s(\tau)$ as a function of frequency in the 10 Hz–2 MHz range for the experimental data presented in Fig. 1.

the specimen under test by an equivalent circuit network composed of several resistors and capacitors in parallel [18,20], or R_i–C_i cell, each being characterized by a relaxation time, τ_i, in Eq. (7):

$$\tau_i = 2\pi R_i C_i. \tag{7}$$

The difficulty with such an approach is to be able to define the number of cells and the values of R_i and C_i for each of them. In a heterogeneous material such as cement, the starting powder is not chemically homogeneous and has a wide grain size distribution. Moreover, as soon as the reaction with water proceeds, the hydrates have a chemical composition which depends on various parameters such as setting time, temperature or water partial pressure. With so many variables, it becomes tricky to assess the importance and the value of each contribution to the global electrical response. However, such an approach has already given a very good first insight into the interpretation of electrical data [20].

In our case, we have used an approach based on the largest possible distribution of relaxation times [28,29]. On the basis that the observed data are linear integral transforms of the quantities to be estimated, Provencher proposes the use of a constrained regularization method in order to find the simplest (most parsimonious) solution that is consistent with the experimental data. For a heterogeneous material such as cement, its complex permittivity can be obtained as follows:

$$\varepsilon^* = \varepsilon_\infty - j\frac{\sigma_0}{\omega} + \int_0^\infty \frac{s(\tau)\mathrm{d}\tau}{1 + j\omega\tau}. \tag{8}$$

For a given distribution of relaxation times, $s(\tau)$ represents its weight fraction. σ_0 is the material conductivity at the low frequency end and ε_∞ is the permittivity at high frequency. From Eq. (8), ε' and σ' can be derived as:

$$\varepsilon' = \varepsilon_\infty + \int_0^\infty \frac{s(\tau)\mathrm{d}\tau}{1 + \omega^2\tau^2} \tag{9}$$

$$\sigma' = \sigma_0 + \omega^2 \tau \int_0^{\infty} \frac{s(\tau)\mathrm{d}\tau}{1+\omega^2\tau^2}. \quad (10)$$

ε'_R can be calculated from ε' since $\varepsilon' = \varepsilon'_R \varepsilon_0$ where ε_0 is the dielectric constant of vacuum. $s(\tau)$, σ_0, and ε_∞ can be deduced from a specific procedure, involving a least square approximation of data with an added quadratic form, the regularizor, which ensures that the calculated values are the most representative of the system under test. In order to restrict the complexity of the problem, Provencher advises the replacement of the linear integral by a sum of 100 discrete elements, which is still an adequate solution for a one-dimension problem.

Using Eqs. (9) and (10), it is possible to obtain a very good fit of our experimental data points (Fig. 1). Fig. 2 presents the variations of $s(\tau)$ as a function of frequency. There are two distributions of time constants. The first one is centered between 10 and 100 Hz, and the frequency at the top increases from 20, 30, and 40 Hz when the electrode is Ag, Au, and In–Ga. The second peak starts beyond 63 Hz. It has the largest area and $s(\tau)$ reaches its highest value (5.2 10^{-6}) when the contact electrode is Ag. In order to understand the origin of this contribution, measurements have been carried out at 100 Hz on samples with increasing thicknesses and coated with Ag electrodes. The values of the capacitance deduced from relative permittivity measurements at 100 Hz are reported in Table 1. The capacitance values are in the nanoFarad range. If we estimate from Fig. 1 that for a cement which is 150 h old ε'_R is equal to 25 (value measured at 1 MHz on samples coated with In–Ga electrodes), the calculated capacitance ranges from 11.9 to 4.1 pF when the thickness increases from 6.4 to 18.4 mm. These calculated values are three orders of magnitude lower than the experimental ones. If we refer to the work by Christensen et al. [13], it could be attributed to the "dielectric amplification factor." It could be a combination of a bulk effect mixed with an electrode effect. To summarize, given the ε'_R values (Fig. 1a), the large weight of the peaks for $s(\tau)$ when using Ag electrodes (Fig. 2), the dielectric response corresponds to the electrode–cement interface and is not specific of the material alone. This result is in accordance with other measurements on cement-based materials carried out in this frequency range [13]. Different groups have shown that this range is quite suitable for studying the interface phenomena between the contact electrode and the cement. In this respect, Mason [30] reports results on steel electrodes immersed in cement paste and has demonstrated how it allows to specifically follow corrosion phenomena at the steel–cement interface. Using gold or indium–gallium mix permits reduction of this electrode contribution to the global electrical response.

Table 1
Capacitance values as a function of sample thickness. Case of an aluminous cement, which is 150 h old, coated with Ag electrodes. The experimental values are deduced from ε'_R data at 100 kHz. The calculated values are estimated for the same material with $\varepsilon'_R = 25$

Thickness (mm)	6.4	9.4	12.4	15.4	18.4
Experimental capacitance ($\times 10^9$ F)	4.8	3.4	2.5	1.9	1.5
Calculated capacitance ($\times 10^{12}$ F)	11.9	8.1	6.2	4.9	4.1

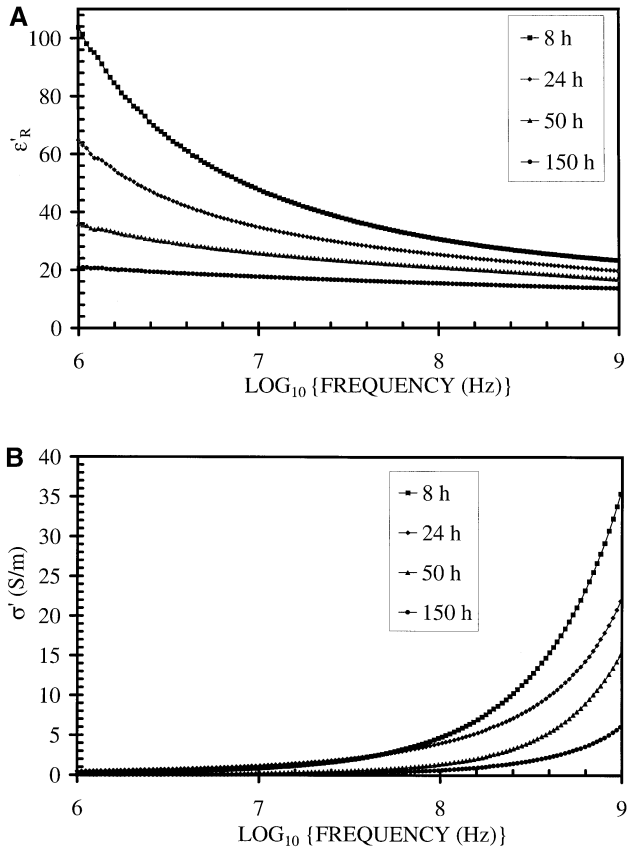

Fig. 3. Variations of ε'_R (a) and σ' (b) in the 1 MHz–1 GHz frequency range for different setting times of the aluminous cement.

Fig. 3 shows the variations of ε'_R and σ' in the 1 MHz–1 GHz frequency range and for different setting times. By applying Provencher's approach, it is possible to get a very good fit of our data points. The corresponding distribution of relaxation times are given in Fig. 4. Peaks at the two ends of the frequency range have been plotted with dotted lines. They should not be considered as truly representative of relaxation phenomena at the cement–water interface for the following reasons: (i) at the high frequency end, multiple reflections of the electromagnetic waves can occur [22], and (ii) at the low frequency end, the peak for $s(\tau)$ can be due to interface effects between the cement disk and the sample holder. Nevertheless, at this low frequency end, the older the cement, the less marked the effect and it has completely disappeared at $t_0 + t_1 = 150$ h. In the rest of the frequency range, the other peaks of $s(\tau)$ are truly representative of the phenomena occurring at the interface between cement particles and water. At $t_0 + t_1 = 8$ h, there is one peak

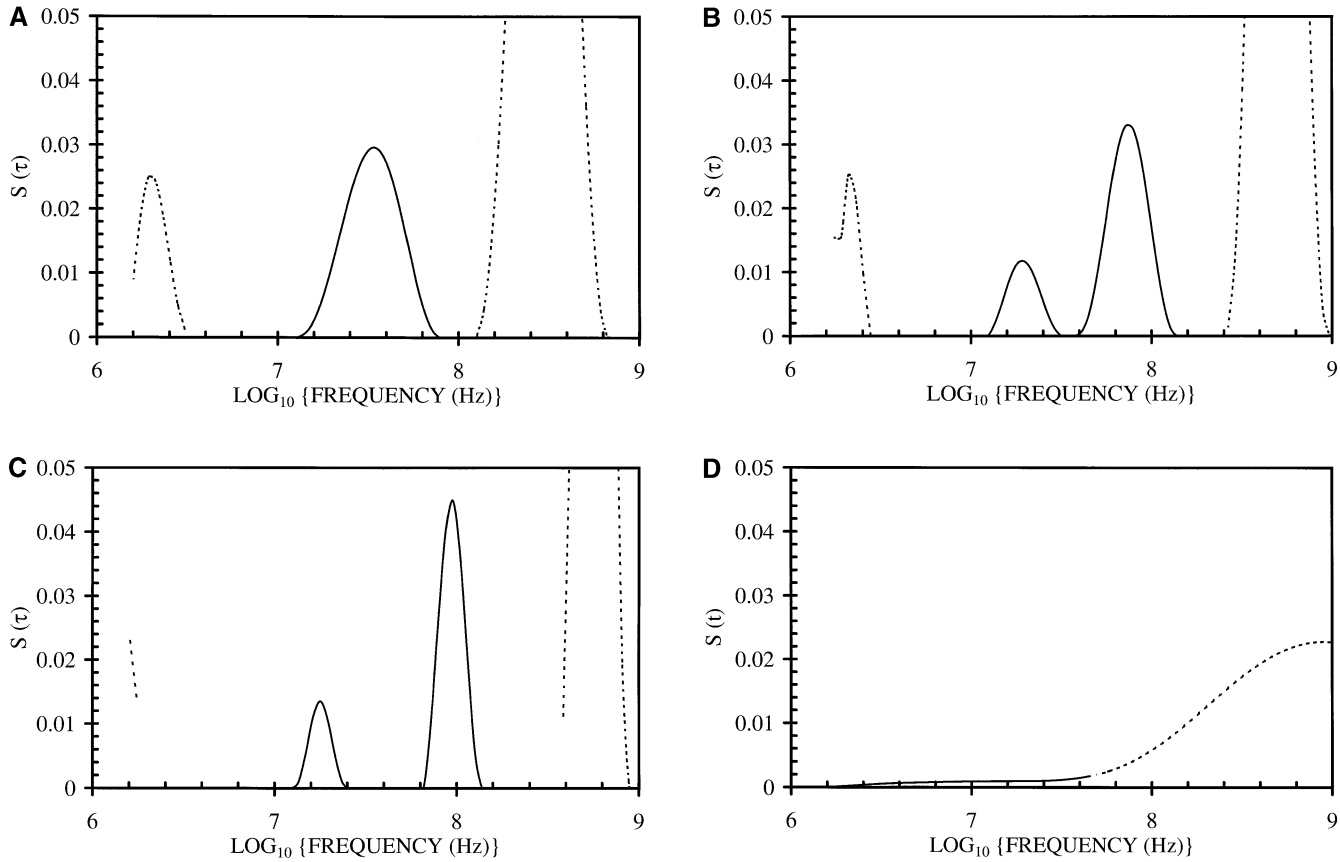

Fig. 4. Variations of $s(\tau)$ as a function of frequency in the 10 Hz–2 MHz range for the experimental data presented in Fig. 3. $t_0 + t_1$ = 8 h (a), 24 h (b), 50 h (c) and 150 h (d).

centered at 34 MHz. At $t_0 + t_1$ equal to 24 and 50 h, there are two peaks whose position and area depend on the setting time. All these peaks are related to the relaxation of water molecules in different environments: free water, water molecules bound via hydrogen bonds to the anhydrous grains, water involved in the formation of crystallized or amorphous hydrates [8,12,16]. Lastly, for the cement which is 150 h old, there is no obvious relaxation phenomenon in this particular frequency range because the water is probably very strongly bound and can no longer relax above 1 MHz.

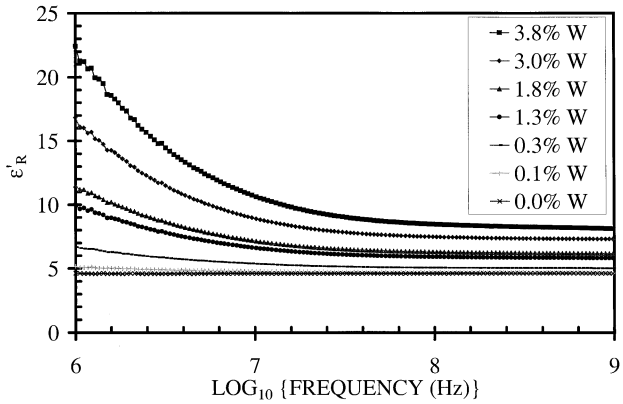

Fig. 5. Variations of ε'_R in the 1 MHz–1 GHz frequency range for the silico-aluminous material containing increasing quantities of water (0 to 3.8 wt.%).

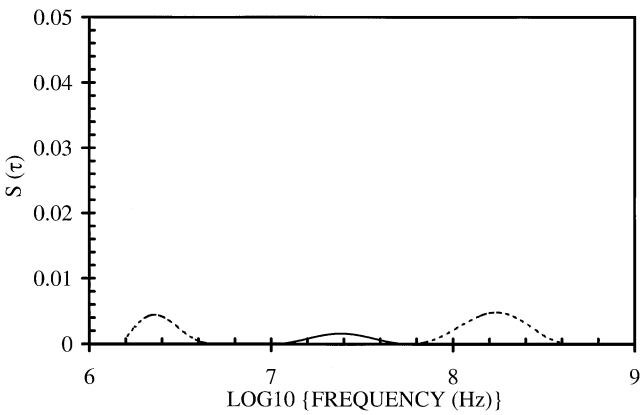

Fig. 6. Variations of $s(\tau)$ as a function of frequency in the 10 Hz–2 MHz range for the silico-aluminous material containing 3.8 wt.% of water.

With respect to the variations of ε'_R as a function of frequency for the silico-aluminous material containing increasing quantities of water, its dielectric response is plotted in Fig. 5. When the water content increases from 0 to 3.8 wt.%, the value of ε'_R at 1 MHz rises from 4.6 to 22.4. It is worth noting that thanks to high frequency measurements, it is possible to track very low amounts of adsorbed water. The distribution of relaxation frequencies for the sample containing 3.8 wt.% of water is plotted in Fig. 6. The distribution is spread between 12 and 50 MHz. These frequencies correspond to the relaxation of the water molecules, which are physically adsorbed at the surface of the pores [26]. The maximum intensity of $s(\tau)$ is of the order of 10^{-3}, which is lower than what is observed in a cement (between 10^{-2} and 5.10^{-2}, see Fig. 4). Therefore, one can assume that in a cement, even if the physical adsorption of water molecules participates to the global dielectric response, its contribution or more precisely its weight in the distribution of $s(\tau)$ is weak compared to the response of water involved into hydrates for instance.

4. Conclusion

Electrical measurements have been carried out on an aluminous cement (CFA from Lafarge) after different setting times (8, 24, 50 and 150 h). An analysis of the data has been carried out using Provencher's approach. In the low frequency range (10 Hz–2 MHz), the electrical response for a material which is 150 h old corresponds to interface phenomena at the cement–electrode interface. At high frequencies (1 MHz–1 GHz), the dielectric behaviour during the first 50 h is characteristic of relaxation of water which is trapped in different environments such as hydrogen bonding to the anhydrous grains, water inside amorphous or crystallized hydrates. Experimental work on pure hydrates is currently in progress and should enable clear separation of these different contributions.

References

[1] A.D. Franklin, Electrode effects in the measurement of ionic conductivity, J Am Ceram Soc 58 (11–12) (1975) 465–473.
[2] J. Ravez, J.P. Bonnet, A. Simon, C. Denage, J.L. Miane, Correlations between processing parameters and relaxation frequencies in $SrTiO_3$-type grain boundary layer ceramics, J Phys Chem Solids 51 (8) (1990) 957–960.
[3] A. Smith, J.F. Baumard, P. Abélard, Ac impedance measurements and V–I characteristics for Co-, Mn-, or Bi-doped ZnO, J Appl Phys 65 (12) (1989) 5119–5125.
[4] F.D. Tamas, E. Farkas, M. Voros, D.M. Roy, Low-frequency electrical conductivity of cement, clinker and clinker mineral pastes, Cem Concr Res 17 (1987) 340–348.
[5] P. Gu, P. Xie, Y. Fu, J.J. Beaudoin, Ac impedance phenomena in hydrating cement systems: The drying-rewetting process, Cem Concr Res 24 (1994) 89–91.
[6] P. Gu, P. Xie, Y. Fu, J.J. Beaudoin, Ac impedance phenomena in hydrating cement systems: Detectability of the high frequency arc, Cem Concr Res 24 (1994) 92–94.
[7] P. Gu, J.J. Beaudoin, Dielectric behaviour of hardened cement paste systems, J Mater Sci Lett 15 (1996) 182–184.
[8] P. Gu, J.J. Beaudoin, Dielectric behaviour of hardened cementitious materials, Adv Cem Res 9 (33) (1997) 1–8.
[9] W.J. McCarter, S. Garvin, N. Bouzid, Impedance measurements on cement paste, J Mater Sci Lett 7 (1988) 1056–1057.
[10] S.S. Yoon, S.Y. Kim, H.C. Kim, Dielectric spectra of fresh cement paste below freezing point using an insulated electrode, J Mater Sci Lett 29 (1994) 1910–1914.
[11] X. Zhang, X.Z. Ding, C.K. Ong, B.T.G. Tan, J. Yang, Dielectric and electrical properties of ordinary portland cement and slag cement in the early hydration period, J Mater Sci 31 (1996) 1345–1352.
[12] Y. El Hafiane, A. Smith, P. Abélard, J.P. Bonnet, P. Blanchart, Dielectric characterization at high frequency of a portland cement at the early stages of hydration, Ceram-Silik 43 (2) (1999) 48–51.
[13] B.J. Christensen, R. Tate Coverdale, R.A. Olson, S.J. Ford, E.J. Garboczi, H.J. Jennings, T.O. Mason, Impedance spectroscopy of hydrating cement-based materials: Measurements, interpretation, and application, J Am Ceram Soc 77 (11) (1994) 2789–2804.
[14] G.M. Moss, B.J. Christensen, T.O. Mason, H.M. Jennings, Microstructural analysis of young cement pastes using impedance spectroscopy during pore solution exchange, Adv Cem Based Mater 4 (1996) 68–75.
[15] R.T. Coverdale, B.J. Christensen, H.M. Jennings, T.O. Mason, D.P. Bentz, E.J. Garboczi, Interpretation of impedance spectroscopy of cement paste via computer modelling, J Mater Sci 30 (1995) 712–719.
[16] N. Miura, N. Shinyashiki, S. Yagihara, M. Shiotsubo, Microwave dielectric study of water structure in the hydration process of cement paste, J Am Ceram Soc 81 (1) (1998) 213–216.
[17] D.E. MacPhee, D.C. Sinclair, S.L. Stubbs, Electrical characterization of pore reduced cement by impedance spectroscopy, J Mater Sci Lett 15 (1996) 1566–1568.
[18] M. Keddam, H. Takenouti, X.R. Novos, C. Andrade, C. Alonso, Impedance measurements on cement paste, Cem Concr Res 27 (8) (1997) 1191–1201.
[19] K. Brantervik, G.A. Niklasson, Circuit models for cement based materials obtained from impedance spectroscopy, Cem Concr Res 21 (1991) 496–508.
[20] D.E. MacPhee, D.C. Sinclair, S.L. Cormack, Development of an equivalent circuit model for cement pastes from microstructural considerations, J Am Ceram Soc 80 (11) (1997) 2876–2884.
[21] J.R. Macdonald, Impedance Spectroscopy, John Wiley & Sons, New York, 1987.
[22] G. Bach, Etude de dispersion en fréquence de la conductivité électrique de suspensions céramiques concentrées, PhD thesis, Limoges University, France, 1998.
[23] W.D. Kingery, H.K. Bowen, H.K. Uhlman, Introduction to Ceramics, John Wiley & Sons, New York, 1976.
[24] C.J. Smithells, Metal Reference Book, Vol. II, Butterworths, London, 1967.
[25] J.W. Fleming, H.M. O'Bryan, Low resistance contacts for semiconducting ceramics, Ceram Bull 55 (8) (1976) 715–716.
[26] C. Ruffet, La conductivité électrique complexe dans quelques roches crustales, PhD thesis, Strasbourg I University, France, 1989.
[27] R. Knight, A. Endres, A new concept in modelling the dielectric response of sandstone: Defining a wetted rock and bulk water system, Geophysics 55 (5) (1990) 586–594.
[28] S.W. Provencher, Comput Phys Commun 27 (1982) 213–227.
[29] S.W. Provencher, Comput Phys Commun 27 (1982) 229–242.
[30] T.O. Mason, private communication.